Forward elastic amplitudes of high-energy pions and kaons on nuclei

C. M. Chen
Saint John's and Saint Mary's Institute of Technology, Tam-Sui Taipei County, Taiwan 25135, Republic of China

Mikkel B. Johnson
Los Alamos National Laboratory, Los Alamos, New Mexico 87545

D. J. Ernst
Department of Physics and Astronomy, Vanderbilt University, Nashville, Tennessee 37235

(Received 2 June 1997)

Experimental elastic angular distributions for pions and kaons in the region of laboratory momentum from 600 to 900 MeV/*c* over the nuclear-Coulomb interference region are analyzed to extract both the real and imaginary part of the forward meson-nucleus scattering amplitude. For pions, results for the total cross sections extracted are smaller than those found from transmission experiments. The real part of the amplitude is found to have an interesting energy dependence. The significance of this result for the behavior of hadrons in nuclei is discussed. For kaons, only qualitative results were obtained due to limited data. [S0556-2813(98)01112-1]

PACS number(s): 25.80.Dj, 25.80.Nv, 24.10.Jv, 13.75.Gx

I. INTRODUCTION

In the scattering of both pions and kaons from nuclei at energies of the order of a GeV, there exists a large angular region in the forward direction where the nuclear and Coulomb amplitudes are of comparable size. This means that it is possible to extract from elastic scattering data in this region both the real and imaginary part of the strong amplitude. Both pieces of information are interesting, as each part of the amplitude contains independent information concerning the dynamics of meson-nucleus reactions.

The density (and, more generally, the density and temperature) dependence of hadron properties is an essential ingredient in understanding such contemporary problems as the transport of hadrons in nuclei and the equation of state of nuclear matter. Pion, kaon, and photon scattering in the GeV region are potentially rich sources of information about these medium modifications because of the ease with which they excite a large class of baryon resonances. By using modern optical model technology, one can make the connection to the resonance amplitude, and perhaps learn how the characteristic properties of the resonances (their masses, total widths, and partial decay widths into pions and nucleons) are changed in the nucleus. The forward scattering amplitude is particularly sensitive to the resonance properties, and by examining the energy dependence of this quantity, one can selectively study the resonances in different energy regions.

Customarily, transmission experiments are used to measure the total cross section which is related to the imaginary part of the forward scattering amplitude. Although the real part of the forward scattering amplitude may, in principle, be determined from transmission measurements [1], this has only been done [2] for the case of pions in the resonance region scattering from medium to heavy nuclei. The imaginary part of the forward scattering amplitude, because it relates to the total cross section through the optical theorem, provides a consistency check between the elastic data and total cross sections extracted from transmission experiments. Exploiting this connection, models for elastic scattering based on the optical potential can be used [3] to produce predictions for total cross sections that can be compared with data [4]. These suggest that the partial widths for the decay of the baryon resonances to the elastic πN channel are increased by a small but significant amount in the nuclei. These results add to a growing body of evidence from kaons [5–7], photons [8,9], and pions [3,10] suggesting that the properties of hadrons are changed in nuclei.

In the analysis of Ref. [3], the effect of the medium on the baryon resonances was accounted for by a change in the total width, taken from Ref. [8], and by a parametrized change in the partial width for decay into the elastic πN channel. The size of the total cross sections could be explained by renormalizing the effective coupling constants of pions to nucleons by about a 15% increase in the average πNN^* coupling constant for the low-lying baryon resonances above the Δ_{33}.

In the meantime, high-energy π^- elastic scattering angular distributions have become available [11]. These precise data add to the rather limited set [4,12–14] of previous data and thus provide additional information relevant to the behavior of baryon resonances in nuclei. It also makes it possible to check for consistency with the previous total cross section data [4] from which the earlier conclusions were drawn [3]. The main purpose of this paper is to determine the imaginary and real parts of the pion-nucleus scattering amplitude by analyzing differential cross section data [11] for pions elastically scattering from ^{12}C. We also examine the possibility of performing a similar analysis for the recently measured [15] kaon-nucleus differential elastic cross sections.

In Sec. II we present the details of our Coulomb-nuclear interference region analysis together with the results of this analysis. We also present some theoretical results for scattering in which the excited baryons are modified by the nuclear medium in order to understand the magnitude that these effects might have on the pion-nucleus forward scattering amplitude. In Sec. III we discuss the significance of the amplitude analysis and draw conclusions.

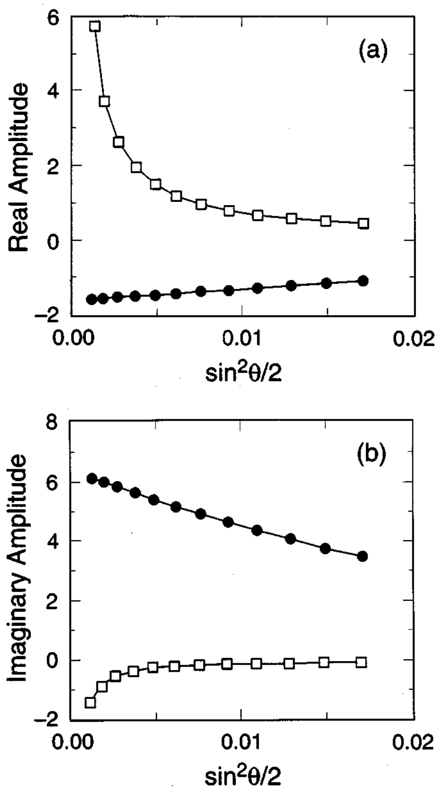

FIG. 1. Real (a) and imaginary (b) parts of the point Coulomb amplitude $f_{c,pt}$ (open squares) and the nuclear amplitude F_N [see Eq. (1)] (solid circles) for π^+ on ^{12}C at 610 MeV/c calculated with ROMPIN plotted against $\sin^2\theta/2$. The points on the curves correspond to angles varying from 4 to 15 degrees in one-degree steps.

II. ANALYSIS

The prospects for determining reliably both the real and imaginary parts of the forward elastic scattering amplitude $F_N(\theta)$

$$F_{\rm el}(\theta)=f_{c,pt}(\theta)+F_N(\theta) \tag{1}$$

are quite good for modern experiments such as that in Ref. [11], where the measurements are made down to angles as small as 5 or 6 degrees with good statistical accuracy. To illustrate this, we show in Fig. 1 the real and imaginary parts of the point Coulomb amplitude $f_{c,pt}(\theta)$ and the nuclear amplitude $F_N(\theta)$ at incident pion momentum of 610 MeV/c calculated with the code ROMPIN [16], which does Fermi averaging of the (resonant plus background) projectile-nucleus amplitudes and incorporates relativistic kinematics. Note that the two amplitudes are of comparable size for angles out to 15 degrees or beyond, so that one can use Coulomb-nuclear interference analysis [17] to determine the real and imaginary parts separately from the data. An inspection of the amplitudes in Fig. 1 shows that in this angular range, the real and imaginary parts of the nuclear amplitude are to a very good approximation linear in $\sin^2\theta/2$. This allows us to represent the amplitudes by four parameters, A_R, B_R, A_I, and B_I:

$$F_N(\theta)=A_R(1-B_R\sin^2\theta/2)+i\,A_I(1-B_I\sin^2\theta/2). \tag{2}$$

We follow Ref. [17] for our amplitude analysis, using the expression in Eq. (2) for the forward scattering amplitude. This expression is inserted into Eq. (1) and the parameters fit to the forward angle experimental differential cross sections. The results are extrapolated to zero degrees to obtain $F_N(0)=A_R+i\,A_I$.

There are two sources of Coulomb corrections that need to be taken into account [17]. The first is a correction for the finite-size extent of the Coulomb interaction, which modifies the real part of $F_N(0)$ by the addition of the quantity

$$-\gamma k R_C^2/3, \tag{3}$$

where $\gamma=ZZ'(e^2/\hbar c)\beta^{-1}$ is the Coulomb parameter, with Z, Z' the charges of the nucleus and projectile, respectively, β is the velocity of the projectile in the center-of-mass (CM) frame, and where $R_C^2=R_N^2+R_p^2$, with R_N and R_p the root-mean-square (rms) charge radii of the nucleus and the projectile, respectively, and k is the CM momentum of the projectile.

The second Coulomb correction is the Coulomb phase σ_ℓ that appears in the partial wave expansion of $F_N(\theta)$. This can be removed by setting

$$F_S(0)=\exp(-i\,\phi_B)F_N(0), \tag{4}$$

where the Bethe phase [18] ϕ_B is found by averaging twice the Coulomb phase over the strong interaction T matrix

$$t_\ell=\exp[i\,\delta_\ell]\sin\delta_\ell, \tag{5}$$

where δ_ℓ is the phase shift of the strong interaction. An explicit expression for the Bethe phase has been obtained in the Gaussian density approximation of West and Yennie [19],

$$\phi_B=\gamma[C+\ln(2k^2(R_s^2+R_C^2)/3)]+2\sigma_0, \tag{6}$$

where C is Euler's constant ($C\sim0.5772$) and R_s is the radius of the strong interaction.

The limitations of the method are discussed in Ref. [17]. The model dependence of the method enters through ϕ_B, since in order to calculate ϕ_B one needs to know the strong interaction, which is the object of the study. Fortunately, as is clear from the result in Eq. (6), ϕ_B is insensitive to the strong interaction. We have further studied the model dependence of ϕ_B for pions on ^{12}C by using Eq. (6) on the one hand (we used $R_N=2.42$ fm for ^{12}C, so $R_C=2.55$ fm, taking $R_p=0.8$ fm for the pion) and by taking the strong interaction phases in Eq. (5) from the model of Ref. [3] on the other. We found that for the energies of interest in this paper, Eq. (6) reproduces ϕ_B in the model of Ref. [3] rather closely taking $R_s=R_N$. The result can be improved, however, by taking R_s to be slightly smaller than R_N (we found that $R_s=2.35$ fm reproduces the results of Ref. [3] rather well); the reduction presumably accounts for the fact that the nucleus is transparent to the pion at high energy and that the Gaussian approximation does not exactly describe the case we are examining. Additionally, as we understand from its definition, the Bethe phase can have an imaginary as well as a real part, but we have again found by explicit calculation, using the theoretical results of Ref. [3] for Eq. (5), that the imaginary part of the Bethe phase is only 1–2% of the real part and hence negligible.

Although we use a model for the strong-interaction radius R_s in the calculation of the Bethe phase, we stress that even a fairly large error in its value has little impact on our final results. This is because the model dependence we have estimated from our tests is very much smaller than the errors introduced by the experimental statistical and systematic errors.

After the corrections for residual Coulomb effects are made, we obtain the strong amplitude $F_S(0)$, to which the optical theorem applies to get the total cross section

$$\sigma_{\rm tot}=\frac{4\pi}{k}\,{\rm Im}\,F_S(0). \tag{7}$$

We are thereby able to determine the strong amplitude at zero degrees and the implied total cross section with reasonable accuracy. The theory of the Coulomb-nuclear interference region is discussed thoroughly in Ref. [17] where the reader may find the underlying theoretical detail.

A. Analysis of π^- scattering data

Our procedure is quite straightforward. Taking the data given in Ref. [11], we fit the parameters A_R, B_R, A_I, and B_I of Eq. (2) to the experimental points for each measured elastic cross section by minimizing χ^2 using the program MINUIT [20]. For this part of the calculation we used the statistical errors. The exact number of data points to be used in the analysis is determined by fitting with the first N data points, then repeating the fit with the first $N+1$ points. When the addition of a point causes an increase in χ^2/N_f (N_f is the number of data points N minus the number of adjustable parameters $N_{\rm par}$), we stop and use the results for the first N points.

For the data from Ref. [11], we find N of 8–10 (corresponding to angles out to 12–15 degrees) satisfies this criterion at each energy. To take the systematic error of 10–12% into account, we perform this analysis three times, once with the data as given in Ref. [11], and once with the data raised by 12%, and once with it lowered by 12%. We have carefully examined the χ-squared space and have found deep and narrow valleys where the fitter would stall and also very flat regions where the fitter would also stall. However, we have in all cases found only one minimum. We did not locate any additional local minima. The resulting χ^2 per degree of freedom N_f is χ^2/N_f=1.6, 0.6, 0.7, and 28, with $N_f=N-N_{\rm par}$ =4,4,4,6 at 610, 710, 790, and 895 MeV/c. This is quite acceptable for all the data sets except the 895 MeV/c case.

TABLE I. The pion-^{12}C amplitudes as defined in Eq. (2) extracted from a fit to the forward angle differential cross sections. The errors given are statistical only.

$k_\pi^{\rm Lab}$ (MeV/c)	A_R (fm)	B_R	A_I (fm)	B_I
610	-2.91 ± 0.31	108 ± 1	6.59 ± 0.06	28.6 ± 0.9
710	0.522 ± 0.06	330 ± 0.1	7.46 ± 0.04	37.0 ± 0.6
790	-1.24 ± 0.04	160 ± 2	7.85 ± 0.04	44.3 ± 0.7
895	-1.67 ± 0.02	116 ± 0.8	8.77 ± 0.01	51.8 ± 0.8

The source of the difficulty here is a combination of very small statistical errors and wiggles in the data that could not be described without very high powers of $\sin^2\theta/2$. We believe that these wiggles cannot be physical and are most likely due to systematic errors which are evidently not adequately accounted for by a uniform renormalization of the data. The results for $\sigma_{\rm tot}$ are 265, 279, 255, and 252 mb, and for Re $F(0)$ we find -3.47, -0.329, -1.87, and -3.53 fm.

A visual examination of the 895 MeV/c data indicates that the first data point is low. We examined the possibility that the results for the forward amplitude might be affected by this one data point by discarding this point and repeating the analysis. We now find that the minimum χ^2/N_f occurs for eight data points ($N_f=4$) just as for the other energies and is equal to 10.4, an improvement over the previous result of 28. This new analysis produced a small change in the imaginary part of the forward amplitude, changing $\sigma_{\rm tot}$ from 239 to 252 mb, and a larger change for Re $F(0)$ from -3.53 to -2.66 fm. We find that the analysis is stable against the removal of an additional point in the forward direction. This is also true for the data at the other energies.

The values for the four parameters of Eq. (2) that were determined from fitting the experimental data of Ref. [11] are shown in Table I. The effect of shifting the data upwards and downwards to account for the systematic errors is very much as expected, namely values that differ from those given in Table I by about 10%. In most of the fits, the parameters A_R, B_R, A_I, and B_I were determined to a few percent by the fitting procedure. The forward scattering amplitudes $F_S(0)$ which result from this analysis are given in Table II.

We have also attempted to perform this analysis utilizing the data from Refs. [12] and [13]. We were not able to find an acceptable fit to these data. Examining the data closely we find that there is a systematic fluctuation in the data. For Ref. [12] (Ref. [13]) the points group themselves into subgroups of six (five) that form a smooth curve, but that these subgroups do not smoothly align with each other. Although the fluctuations between the subgroups are small, we were not

TABLE II. Coulomb corrections [see Eqs. (4) and (6)] and the final values for the strong amplitudes at zero degrees for pion ^{12}C scattering. The first error is statistical, and the second systematic.

$k_\pi^{\rm Lab}$ (MeV/c)	$-\gamma k R_C^2/3$ (fm)	ϕ_B	Re $F_S(0)$ (fm)	σ_T (mb)
610	0.271	-0.130	$-3.47\pm0.31\pm0.17$	$265\pm2\pm15$
710	0.309	-0.141	$-0.329\pm0.06\pm0.09$	$279\pm1\pm16$
790	0.338	-0.148	$-1.87\pm0.04\pm0.31$	$255\pm1\pm15$
895	0.376	-0.159	$-2.66\pm0.05\pm0.23$	$252\pm1\pm14$

TABLE III. The forward amplitude [see Eqs. (8) and (9)] for K^+ scattering as determined from the fit to the data of Ref. [15]. Only statistical errors are included.

$10^4\alpha$	$A_{I,C}$ (fm)	$A_{I,Li}$ (fm)	$10^{-4}B_R$	B_I
1.17±1.18	4.67±0.36	2.2±0.11	4.95±4.99	28.73±1.65

able to find a suitable algorithm for selecting the number of data points that would provide a stable answer. We note that the data is taken for a group of angles for each positioning of the spectrometer. This systematic fluctuation in the data is most likely related to each actual physical angular setting of the spectrometer.

B. Analysis of K^+ scattering data

In Ref. [15], angular distribution data is obtained for K^+ scattering from ^{6}Li and ^{12}C at 715 MeV/c. The amplitude analysis of this data proceeds exactly as it did for the pion. We have taken the first four points (out to 22 degrees) to encompass the Coulomb-nuclear interference region. We found from the theoretical calculations that such an interval, for pions, would surely contain significant $\sin^4\theta/2$ terms. The angular variation of the K^+-nucleus amplitude is weaker than it is for pions (due to the weaker interaction and fewer partial waves in the K^+-nucleon scattering amplitude) and thus permits a larger angular region to be used.

The fact that there are four parameters to be determined for the Coulomb-nuclear interference measurement is problematic, because there are only four data points in the Coulomb-nuclear interference region [15] and each has significant statistical and systematic errors. We find that this number and quality of the data is insufficient to make a meaningful χ^2 fit of the four parameters in Eq. (2). The only way, short of additional data in the Coulomb-nuclear interference region for K^+, to get a determination of the parameters is to make assumptions that relate the parameters for ^{12}C to those for ^{6}Li and to fit to the combined data set. The following assumptions permit a fit of this type, but conclusions drawn from a fit based on these assumptions should be treated as quite tentative:

(1) The parameters B_R and B_I are the same for ^{6}Li and ^{12}C. The reason for this is that the shape of the angular distribution, in contrast to the overall magnitudes, are expected to be determined by the geometry of the nucleus. This is true both in the Born approximation and in the diffractive limit. Note that the radii of the two nuclei are the same to about 4%. Thus, in the limit that the two densities differ only in their overall norm, we expect these parameters to be quite similar.

(2) $A_R(^{12}\mathrm{C})/A_I(^{12}\mathrm{C}) = A_R(^6\mathrm{Li})/A_I(^6\mathrm{Li}) = \alpha$. This assumption would be expected to hold if the amplitudes were proportional to a medium modified two-body amplitude times the density, such as would occur for nucleons uniformly distributed in boxes of the same radii and to the extent that the medium modifications affect the real and imaginary parts of the scattering amplitudes in the same way. The fact that the real and imaginary parts are slowly varying functions of energy supports this assumption. Multiple scattering, which we expect to be larger in ^{12}C than ^{6}Li, would modify this relation. We can check the importance of multiple scattering using the lowest-order optical potential. In the model of Ref. [7], we find $\alpha = -0.596$ for K^+ on a ^{12}C target at incident momentum of 715 MeV/c, and $\alpha = -0.528$ on a ^{6}Li target, indicating that our scaling assumption, although not exact, is reasonable in this case.

Note that these assumptions do not necessarily rule out the possibility that the medium effects in ^{6}Li and ^{12}C are different. Presumably, if medium effects exist, they would be reflected in different overall strengths for the amplitudes, as reflected in the parameters $A_{I,\mathrm{C}}$ and $A_{I,\mathrm{Li}}$ [see Eqs. (8) and (9) below].

With these two assumptions, the amplitude in Eq. (2) for K^+ would become, for ^{12}C

$$F_N(^{12}\mathrm{C},\theta) = \alpha A_{I,\mathrm{C}}(1 - B_R\sin^2\theta/2) + i A_{I,\mathrm{C}}(1 - B_I\sin^2\theta/2), \tag{8}$$

and for ^{6}Li,

$$F_N(^6\mathrm{Li},\theta) = \alpha A_{I,\mathrm{Li}}(1 - B_R\sin^2\theta/2) + i A_{I,\mathrm{Li}}(1 - B_I\sin^2\theta/2), \tag{9}$$

for a total of five parameters (α, $A_{I,\mathrm{C}}$, $A_{I,\mathrm{Li}}$, B_R, and B_I) to be determined by the two data sets together. Since there are eight data points within the Coulomb-nuclear interference region, the χ^2 minimization procedure will give a meaningful test for the assumptions made above.

We have made the analysis based on Eqs. (8) and (9) above, and the results are given in Table III for the ^{6}Li and ^{12}C at 715 MeV/c incident laboratory momentum. The correction for the Coulomb interaction proceeds just as in the case for pions, and the results are given in Table IV. We have taken the Coulomb radius R_π=0.8 fm for the kaon as well as for the pion, so R_C is the same as for the pion in the case of ^{12}C. For ^{6}Li, we take R_N=2.56, so R_C=2.68 for K^+ on ^{6}Li.

Our fit to the combined data set gives χ^2/N_f to be 3.8. Our assumptions thus do not obviously contradict the data. The errors on the total cross section are about 8 and 5%, respectively, for ^{12}C and ^{6}Li. The real parts of the forward scattering amplitudes are, however, not so well determined, having 100% errors. About all one can say about the real parts is that they are positive and small. We do not believe that the quality of the results combined with the unknown dependence on our assumptions merits an analysis that would also include the systematic error.

TABLE IV. Coulomb corrections [see Eqs. (4) and (6)] and final values for the strong amplitude for K^+. Only statistical errors are included.

Target	$-\gamma k R_C^2/3$ (fm)	ϕ_B	Re $F_S(0)$ (fm)	Im $F_S(0)$ (fm)
^{12}C	−0.411	0.216	0.598±0.598	4.65±0.36
^{6}Li	−0.211	0.109	0.0288±0.0288	2.21±0.11

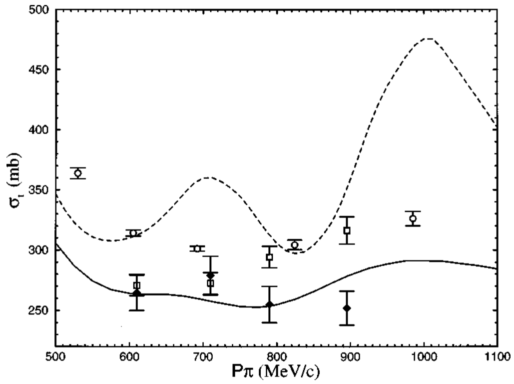

FIG. 2. Total cross sections for π^- on ^{12}C as derived here and given in Table II compared with earlier determinations. The results of the present analysis (solid diamonds) are plotted with the data of Clough (Ref. [4]) (open circles) and the results of Takahashi (Ref. [11]) (open squares). The dashed curve is the free isospin averaged pion-nucleon total cross section times 12. The solid curve is the result of a calculation utilizing a covariant optical potential which includes Fermi averaging and multiple scattering.

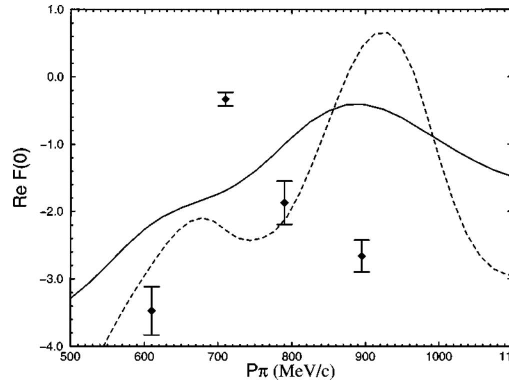

FIG. 3. Re $F(0)$ for π^- on ^{12}C as derived here and given in Table II. The curves are the same as in Fig. 2.

C. Comparisons to earlier data and to theory

Because total cross sections for pions in the GeV range of energies have been obtained from transmission experiments, we are able to compare the imaginary part of the empirical forward scattering amplitudes determined from the Coulomb-nuclear interference analysis to independent determinations using the optical theorem, Eq. (7). We will do this for both pions and kaons in this subsection.

Additionally, for the case of pions, we will compare our empirical results to theoretical calculations based on existing models that have been proposed to understand pion scattering data in the GeV energy region. As there have been no previous experimental determinations of the real part of the amplitude, there are no independent measurements with which we can compare this quantity.

1. Pions

In Fig. 2 we compare our total cross section results for pions with previous measurements. We see that the forward amplitude (solid diamonds) that we have extracted from the data of Ref. [11] implies total cross sections significantly smaller than those [4] extracted from transmission experiments (open circles). This conclusion is consistent with the results of Ref. [11] (open squares), at least for the two lower momenta (610 and 710 MeV/*c*), with which our results are statistically consistent. However, our results at the two higher energies are not only smaller than those of the transmission measurements, but also quite a bit smaller than the total cross sections obtained by the analysis in Ref. [11].

The source of the difference between our results and those of Ref. [11] is the different fitting procedures used. In Ref. [11], the parameters of the model were determined by minimizing χ^2 using data over the *entire* angular range, whereas in our work only the forward angle data was used. From examining their fits [11], it is clear that large- and small-angle data are not capable of being fit simultaneously. As a result, their fit to the (relevant) forward angle data is much poorer than ours, and this accounts for the differences seen in Fig. 2. Generally speaking the large-angle data, which is from two to four orders of magnitude smaller than the measurements of the most forward-angle data, is sensitive to small effects and hard to fit in models. The relevance of the back-angle data to the total cross section is obscure in phenomenological models (such as the one we are using as well as that of Ref. [11]) that leave out higher-order terms in the optical potential.

We also present in Fig. 2 two curves. The dashed curve is the spin and isospin averaged free two-body total cross section multiplied by 12. The two peaks in this curve correspond to the two groups of excited baryons which are present in this energy regime. The solid curve is the result of a first-order optical potential calculation without medium modifications to the resonances utilizing the code ROMPIN [16]. We see that the Fermi averaging over the momentum of the struck nucleon plus the broadening caused by multiple scattering greatly removes the peak structure in the cross section.

In Ref. [3], the discrepancy between the solid curve and the data of Ref. [4] was interpreted as evidence for a substantial renormalization of the average πNN^* coupling constant of all resonances lying in the region between 600 and 900 MeV/*c*. With the smaller total cross sections that we have extracted here, there is no longer evidence for such a large uniform renormalization. In fact, the theoretical curve is reasonably consistent with the data. The experimental point at 710 MeV/*c* lies slightly above the curve. Since this is near the peak of the D_{13} resonance, a very tentative conclusion might be that its coupling to the pi-nucleon channel should be increased a small amount.

The real part of the pion-nucleon scattering amplitude, unlike the imaginary part, has the feature that it is composed of contributions from individual resonances that are not all positive definite; the real part of a resonant amplitude changes sign as the energy passes through the resonance. This implies that a measurement of the real part of the pion-nucleus amplitude provides different information from that provided by the total cross section, and that the real part complements the imaginary part for the purpose of separating the contributions from the overlapping resonances in the medium. The real part of the amplitude that we have extracted is given in Table II and pictured in Fig. 3. The experimental results are interesting because they have a strong energy dependence, peaking at an incident pion momentum of about 700 MeV/*c*. For comparison, we show the free two-body amplitude times 12 (dashed curve) and the theoretical

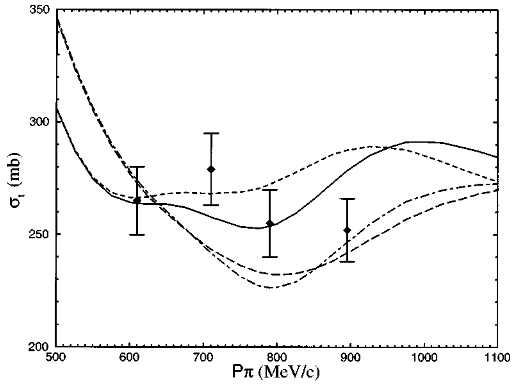

FIG. 4. The total cross section for π^- on ^{12}C as derived here (diamonds). The solid curve is the same as in Fig. 3, the results of the optical model calculation. The dashed curve includes the additional broadening of the baryon resonances according to Refs. [3] and [8]. The dotted curve is the same as the solid curve except the mass of the F_{15} resonance has been lowered by 50 MeV. The dot-dash curve is the same as the dashed curve except the mass of the F_{15} resonance has been lowered by 50 MeV.

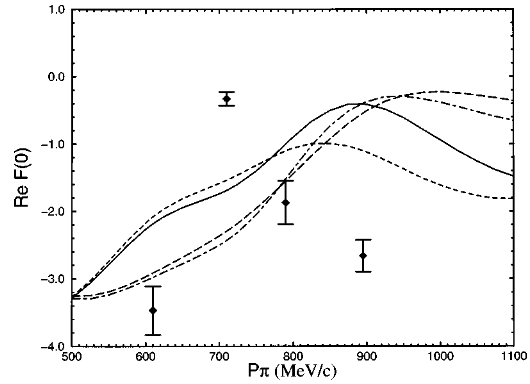

FIG. 5. The same as Fig. 4 except Re $F(0)$ is presented.

results of ROMPIN without medium modifications of the resonances (the solid curve). The free two-body amplitude has two bumps, the one lower in energy appearing in the region of the D_{13} resonance, and the higher one appearing in the region of the F_{15} resonance. Note that the free amplitude even changes sign in the region of the F_{15} resonance. Fermi averaging and multiple scattering, given by the solid curve, wash out much of this structure. Note that there is still a bump in the region of the F_{15} resonance, but that the amplitude is now negative over the entire energy region.

The peaking of the experimental real part occurs at a considerably lower energy than the peak in our solid curve, and we have tried to understand this discrepancy. We have tried variations of our data analysis. For example removing the first data point from our Coulomb-nuclear interference analysis. In all cases, the results we find remain stable, but we do find that the χ^2 surface is very flat. We have searched for a local minimum that would produce a larger negative Re $F(0)$ at 710 MeV/c but did not find one. The result appears to be very stable. The errors shown in Figs. 2 and 3 are dominated by the systematic normalization errors in the differential cross sections, which we have accounted for by refitting the data after raising and lowering the cross sections by the appropriate amount. The slope of the data is very important in our analysis, since it is necessary to extrapolate the results into a zero angle. If the slope of the data were in error (we have no reason to believe that it is) then this could result in much different values of $F_S(0)$.

In Figs. 4 and 5 we present the data for σ_{tot} and Re $F(0)$ as extracted in this work together with several theoretical curves. The issue we wish to examine is how sensitive is $F(0)$ to medium modifications of the excited baryons. The solid curve in both figures is the result from ROMPIN without medium modifications to the resonances. In Ref. [3] we increased the in-medium widths of the resonances according to the results of Ref. [8]. Applying this model gives the results pictured as the dashed curves in Figs. 4 and 5. We do not employ the increase in the coupling constants suggested in Ref. [3] as our analysis here (see Fig. 2) indicates that this is not necessary. There is a sufficient difference between the solid and dashed curves for both the real and imaginary parts of $F(0)$ that such an effect could be detectable. We have also examined the sensitivity to the in-medium masses of the resonances by repeating the above two calculations with the mass of the F_{15} lowered by 50 MeV, the value of the shell-model potential at the middle of a nucleus. The ROMPIN curve with the shifted F_{15} mass is the dotted curve in both figures. For σ_{tot} the peak near 1 GeV/c is shifted downwards by about 50 MeV, as expected, and there is a substantial enhancement of the total cross section in the region between 600 and 900 MeV/c. For Re $F(0)$ the peak near 1 GeV/c is also shifted downwards in energy, and the magnitude of Re $F(0)$ is enhanced [$F(0)$ becomes more negative] from 800 to 1100 MeV/c. For the results which have the additional medium broadening taken from Ref. [8] (dashed curves), the change in mass of the F_{15} (dot-dashed curves) has relatively little effect. If the widths of these resonances are as broad as implied by Refs. [3] and [8] the effect of mass shifts will be difficult to extract.

The type of medium effects we have examined here do not appear to be able to reproduce the experimental results. In particular, the peak of Re $F(0)$ near 700 MeV [more correctly described, this is a dip in the magnitude of Re $F(0)$] is a feature that is not in the theory. This intriguing result should be verified by data taken at closely spaced energies.

2. Kaons

The forward scattering amplitudes for K^+ are given in Table V, where they are compared to results of independent measurements of total cross sections [21] extracted from transmission experiments. The agreement with the previous data is rather satisfactory and lends support to the parametrization we have chosen in Eqs. (8) and (9). The value for Re $F(0)$ for the kaon which we here extracted cannot be

TABLE V. Comparison of the results of this paper for K^+ to total cross sections as extracted from transmission experiments. Only statistical errors are given.

Target	Im $F_S(0)$ (fm)	σ_T (this work)	σ_T (previous)
^{12}C	4.65±0.36	173±14	178.66±0.72
^{6}Li	2.21±0.11	88±4	87.05±0.64

compared to the results presented in Ref. [22]. There, this same data was analyzed utilizing a phenomenological second-order optical potential. In order to find a consistent interpretation of the total and elastic differential cross sections for a variety of nuclei simultaneously, the differential cross sections had to be renormalized substantially. This would necessarily alter the value of $F(0)$ that would result.

III. DISCUSSION AND CONCLUSION

We have argued that the forward-angle strong meson-nucleus amplitude is interesting because properties of hadrons in the nuclear medium can be addressed from knowledge of this quantity. The relevant quantity to be measured is the differential cross section in the Coulomb-nuclear interference region from which the real and imaginary parts of the forward scattering amplitude can be extracted by a simple model-independent fitting procedure that we apply to existing data. Coulomb-nuclear interference, which is significant over a measurable angular region, allows the extraction of both pieces of the forward amplitude separately. The uncertainty arising from our parametrization of the amplitude is significantly less than the uncertainty arising from the experimental errors. Our main interest has been in determining this amplitude for existing data, rather than its interpretation in terms of the medium modification of hadrons, which will be the subject of a future publication.

Pion-nucleus scattering is of particular interest because of its underlying resonance structure. For a single isolated resonance, data over the peak of the resonance can be used to determine its in-medium properties. Such is the case for the Δ_{33} resonance [23]. Determining the in-medium properties resonances above the Δ_{33} requires that the energy dependence of the pion-nucleus amplitude be known over a larger region due to the fact that these resonances are overlapping. Knowledge of the real part of the amplitude, which we find to have a striking energy dependence, will be particularly useful in this case. We have shown that the energy dependence of the real and imaginary parts of the forward amplitude provide complementary information about the behavior of the resonances in the nucleus by examining theoretical models.

As we have seen for pions (Fig. 2), the values of the total cross section obtained from our analysis disagree with the earlier transmission measurements of the same quantity. We have discussed several possible reasons for this discrepancy, which we believe to be of experimental origin. In view of this disagreement, additional independent measurements of the total cross sections should be performed at modern facilities. Furthermore, because of the interest in the real part of the forward elastic scattering amplitude, strengthened by the striking energy variation in Table II and Fig. 3, it would be useful to have more measurements of the angular distribution at finer energy steps to both confirm the results we have extracted from the data of Ref. [11] and to pin down the shape of the energy dependence. It would be useful to have these data up to several GeV, covering the full range where the baryon resonances occur. The region over which the Coulomb-nuclear interference analysis can be performed is to lowest approximation a region of fixed q^2, assuming the two-body amplitude is not particularly energy dependent. Thus the angular region of 5–15 degrees at one GeV would become approximately 2.5–7.5 degrees at two GeV. Data for both charges of the pion would also be most useful.

For K^+, it is important to have more and higher statistics measurements in the Coulomb-nuclear interference region (between 5 and 20 degrees) so that the amplitude analysis can be carried out without additional assumptions. The existing data for total cross sections as derived from transmission experiments indicate that the kaon-nucleon coupling is effectively increased for the nucleon in a nucleus. Having the forward angle K^+ amplitude would provide an additional independent constraint on any theoretical model.

A complete picture requires data from other final channels and a theory general enough to incorporate this data into the analysis. Data on quasielastic kaon [24] scattering and quasielastic pion scattering, both with [25] and without [26] charge exchange, have been measured with additional data coming from KEK. Exclusive π^+ and π^- elastic and charge exchange data and K^+ charge exchange would also be useful in understanding the isospin dependence of any missing piece of physics. Additional data is being taken at KEK and should be available soon.

ACKNOWLEDGMENTS

The work of D.J.E. was supported in part by the U.S. Department of Energy under Grant No. DE-FG02-96ER40975. The work of C.M.C. was supported in part by the ROC National Science Council under Grant No. NSC 86-2112-M-129-001. M.B.J. and C.M.C. would like to thank Vanderbilt University for their hospitality during part of this work, and C.M.C. and D.J.E. would like to thank the Los Alamos National Laboratory for their hospitality during part of this work.

[1] M. D. Cooper and M. B. Johnson, Nucl. Phys. **A260**, 352 (1976).
[2] R. H. Jeppson *et al.*, Phys. Rev. C **27**, 697 (1983).
[3] C. M. Chen, D. J. Ernst, M. F. Jiang, and M. B. Johnson, Phys. Rev. C **52**, R485 (1995).
[4] A. S. Clough *et al.*, Nucl. Phys. **B76**, 15 (1974).
[5] P. B. Siegel, W. B. Kaufman, and W. R. Gibbs, Phys. Rev. C **30**, 1256 (1984).
[6] G. E. Brown, C. B. Dover, P. B. Siegel, and W. Weise, Phys. Rev. Lett. **26**, 2723 (1988).
[7] C. M. Chen and D. J. Ernst, Phys. Rev. C **45**, 2019 (1992); M. F. Jiang, D. J. Ernst, and C. M. Chen, *ibid*. **51**, 857 (1995).
[8] L. A. Kondratyuk, M. I. Krivoruchenko, N. Bianchi, E. De Sanctis, and V. Muccifora, Nucl. Phys. **A579**, 453 (1994).
[9] W. A. Alberico, G. Gervino, and A. Lavagno, Phys. Lett. B **321**, 177 (1994).

[10] M. Arima, K. Masutani, and R. Seki, Phys. Rev. C **51**, 285 (1995).
[11] T. Takahashi *et al.*, Phys. Rev. C **51**, 2542 (1995); T. Takahashi, Ph.D. thesis, Department of Physics, Kyoto University, 1995.
[12] D. Marlowe *et al.*, Phys. Rev. C **25**, 2619 (1982).
[13] G. Kahrimanis *et al.*, Phys. Rev. C **55**, 2533 (1997).
[14] M. W. Rawool-Sullivan *et al.*, Phys. Rev. C **49**, 627 (1994).
[15] R. Michael *et al.*, Phys. Lett. B **382**, 29 (1996).
[16] D. R. Giebink and D. J. Ernst, Comput. Phys. Commun. **48**, 407 (1988).
[17] M. D. Cooper, M. B. Johnson, and G. B. West, Nucl. Phys. **A292**, 350 (1977).
[18] H. A. Bethe, Ann. Phys. (N.Y.) **3**, 190 (1958).
[19] G. B. West and D. R. Yennie, Phys. Rev. **172**, 1413 (1968).
[20] MINUIT, CERN Program Library Entry D506.
[21] E. Mardor *et al.*, Phys. Rev. Lett. **65**, 2110 (1990); R. A. Krauss *et al.*, Phys. Rev. C **46**, 655 (1992); R. Sawafta *et al.*, Phys. Rev. B **307**, 293 (1993); R. Weiss *et al.*, Phys. Rev. C **49**, 2569 (1994).
[22] C. M. Chen, D. J. Ernst, and M. B. Johnson, Phys. Rev. C (submitted).
[23] L. S. Kisslinger and W. Wang, Phys. Rev. Lett. **30**, 1071 (1973); Ann. Phys. (N.Y.) **99**, 374 (1976); M. Hirata, J. H. Koch, F. Lenz, and E. J. Moniz, Phys. Lett. **70B**, 281 (1977); Ann. Phys. (N.Y.) **120**, 205 (1979); E. Oset and W. Weise, Nucl. Phys. **A329**, 365 (1979); M. B. Johnson and D. J. Ernst, Ann. Phys. (N.Y.) **219**, 266 (1992); C. M. Chen, D. J. Ernst, and M. B. Johnson, Phys. Rev. C **47**, R9 (1993).
[24] C. M. Kormanyons *et al.*, Phys. Rev. Lett. **71**, 2571 (1993); Phys. Rev. C **51**, 669 (1995); C. M. Kormanyons and R. J. Peterson, Nucl. Phys. **A585**, 113 (1995).
[25] R. J. Peterson *et al.*, Phys. Lett. B **297**, 238 (1992); J. Ouyang *et al.*, Phys. Rev. C **47**, 2809 (1992); **48**, 1074 (1993); J. D. Zumbro *et al.*, Phys. Rev. Lett. **71**, 1796 (1993).
[26] J. E. Wise *et al.*, Phys. Rev. C **48**, 1840 (1993).